

## Exciton capture and losses in a stacked submicron array of sidewall quantum wires on patterned GaAs(311)A substrates

U. Jahn, R. Nötzel, J. Ringling, H.-P. Schönherr, H. T. Grahn, and K. H. Ploog  
Paul-Drude-Institut für Festkörperelektronik, Hausvogteiplatz 5-7, D-10117 Berlin, Germany

E. Runge

Institut für Physik, Humboldt Universität zu Berlin, Hausvogteiplatz 5-7, D-10117 Berlin, Germany

(Received 24 February 1999)

The optical properties of stacked GaAs/(Al,Ga)As quantum wire arrays, with a 0.5  $\mu\text{m}$  lateral period fabricated by molecular beam epitaxy on patterned GaAs(311)A substrates, have been investigated. We observe an unexpectedly high quantum wire related contrast in the lateral distribution of the cathodoluminescence (CL) intensity, in particular at 300 K. The temperature dependence of this contrast as well as of the integrated CL intensities in the quantum wires and connecting quantum wells, reveals the loss mechanisms, which cause a reduction of the exciton transfer efficiency from the well into the wire regions. For low and intermediate temperatures, exciton localization and nonradiative recombination within the quantum well regions contribute to the decrease of the transfer efficiency. Near room temperature, the vertical escape of carriers, in particular out of the quantum well regions into the (Al,Ga)As barriers, is the limiting process. Within the framework of a detailed model, we determined the transfer time and the ratio of the radiative recombination times in the well and wire regions by combining the spatially resolved CL measurements with time-resolved photoluminescence spectroscopy. [S0163-1829(99)12539-6]

### I. INTRODUCTION

The electronic properties of single quantum wires (Qwire) as well as of Qwire arrays have been widely investigated.<sup>1-9</sup> Most studies in this field have been performed on crescent-shaped Qwires grown on V-groove-patterned GaAs(100) substrates.<sup>1-5,7,9</sup> Since in array structures the lateral width of the connecting quantum well (Qwell) regions is usually much larger than the one of the Qwire regions, a fast transfer of excited carriers from the Qwells towards the Qwires is necessary for a high capture efficiency of the Qwires. Therefore, the transfer time  $\tau_t$  of excitons generated in the Qwells is a crucial quantity for a successful application of such Qwire arrays in device structures. The ratio  $R_{PL} = I_{PL}^W / I_{PL}^R$ , where  $I_{PL}^W$  and  $I_{PL}^R$  are the spatially integrated photoluminescence (PL) or cathodoluminescence (CL) intensities of the Qwell and Qwire spectra, is usually applied to estimate the exciton transfer efficiency.<sup>2,7</sup> Such an approach, however, neglects nonradiative recombination in the Qwell and Qwire regions as well as other loss mechanisms. As found previously in several works,<sup>10-13</sup> nonradiative decay channels can actually be of importance for the recombination dynamics even at low temperatures. Therefore, the measured ratio  $R_{PL}$  probably reflects an overestimated transfer efficiency for the whole temperature range. In Ref. 2, e.g., the authors estimated a value of  $\tau_t < 0.1$  ps for a 240 nm period Qwire array, which is extremely fast. However, if the diffusivity ( $D$ ) and lifetime ( $\tau$ ) of excitons in thin Qwells—as determined by Hillmer *et al.*<sup>14</sup> and Gurioli *et al.*<sup>10</sup>—are taken into account, exciton diffusion lengths ( $L$ ) on the order of 100 nm are obtained at low temperatures. This is consistent with the value of  $L = 130$  nm found by Grundmann *et al.*<sup>4</sup> within the connecting Qwells of a Qwire array exhibiting a well width

of 2 to 3 nm. Hence, the distance, which can be covered by the excitons during their lifetime, is of similar magnitude as the lateral width of the Qwell regions. From this point of view, it is not expected that the transfer time differs by orders of magnitude from the lifetime even for a periodicity of the Qwires of a few 100 nm.

Recently, we reported on the successful growth of a Qwire array with 0.5  $\mu\text{m}$  periodicity on patterned GaAs(311)A substrates, which results in a less complex structural arrangement compared with V-groove structures.<sup>15</sup> While the latter consists of the crescent Qwire and various Qwell regions, which differ in thickness and orientation, the Qwires based on the GaAs(311)A substrate appear as thicker, lens-shaped regions, which are laterally connected with each other by thinner, almost smooth Qwell regions. In our system, the luminescence response solely consists of two well separated spectral lines, which are assigned to the Qwire and Qwell regions. The energy difference between the Qwire and Qwell luminescence lines indicates a lateral confinement potential of 210 meV. Furthermore, the exciton transfer between the Qwell and Qwire regions is very efficient resulting in high luminescence intensities of the Qwire even at room temperature. Therefore, the present Qwire structure allows for a comprehensive study of the exciton capture, recombination dynamics, and escape behavior, which is important for a basic understanding as well as for a further optimization of Qwire array systems with regard to device applications.

In this work, we present experimental results of spatially resolved CL investigations between 5 and 300 K of a stacked sub- $\mu\text{m}$ -pitch Qwire array. We find that nonradiative recombination within the Qwell regions cannot generally be neglected. Furthermore, we observe that re-emission of excitons, in particular out of the Qwell regions into the (Al,Ga)As barrier material, results in an increasing reduction

of the transfer efficiency, when the temperature is increased to 300 K. A model shows that a combination of spatially and time-resolved luminescence experiments can yield information about the excitonic transfer time and the ratios of the radiative recombination rates in the Qwire and Qwell regions.

The paper is organized as follows. In Sec. II, the experiments are described. The obtained results are discussed in Sec. III, where in the first and second subsections data of spatially resolved CL investigations obtained at low and high temperatures are presented, respectively. The third subsection deals with the time-resolved PL results. Finally, in the fourth subsection, a model is discussed. Section IV contains a summary.

## II. EXPERIMENT

The GaAs(311)A substrate was patterned with a  $0.5 \mu\text{m}$  pitch periodic grating by holographic lithography and subsequent dry etching to a depth of 15 nm. The samples were cleaned in concentrated  $\text{H}_2\text{SO}_4$ , and the native oxide was removed in the preparation chamber by atomic hydrogen irradiation before loading them into the growth chamber. The following layer sequence was deposited by molecular beam epitaxy (MBE) on top of the patterned substrate: a 50 nm GaAs buffer layer, 50 nm  $\text{Al}_{0.5}\text{Ga}_{0.5}\text{As}$ , a stack of 3 Qwells consisting of 3 nm thick GaAs well and 10 nm thick  $\text{Al}_{0.5}\text{Ga}_{0.5}\text{As}$  barrier layers, 50 nm  $\text{Al}_{0.5}\text{Ga}_{0.5}\text{As}$ , and a 20 nm thick GaAs cap layer. A reference quantum well was grown side by side on a planar GaAs (311)A substrate, which results in a nominal thickness of the well layer of 3 nm.

CL spectra, line profiles, and images were obtained in a scanning electron microscope (SEM) equipped with an Oxford mono-CL and He-cooling stage for temperatures ranging from 5 to 300 K. The time-resolved PL measurements were performed using the second harmonic of a modelocked, frequency tunable Ti:sapphire laser (Coherent Mira) with a pulse width of about 150 fs and a repetition rate of 76 MHz as the excitation source. The PL signal was dispersed by a 0.22 m monochromator and recorded by a streak-camera system (Hamamatsu) in syncscan operation.

## III. RESULTS AND DISCUSSION

### A. Spatially resolved CL

Figure 1 shows the CL spectrum and the CL image of the quantum wire array at 5 K. As discussed in Ref. 15, the CL lines centered at 1.61 and 1.83 eV originate from the Qwire and Qwell regions, respectively. The lateral intensity distribution exhibits a regular, stripe-like pattern, which clearly reflects the grating period. For the upper and lower part of the CL image, the detection energy was set to the spectral position of the Qwell and Qwire emission, respectively. Compared with the lateral CL intensity distribution of the upper part, the lower one exhibits a shift perpendicular to the wires by half a period of the wire array. This confirms that the respective CL arises from spatially separated, neighboring regions. The fact that we are able to clearly resolve the Qwire array by CL imaging already indicates an incomplete transfer of excitons from the Qwell to the Qwire regions. For a complete transfer of Qwell excitons, we would not expect

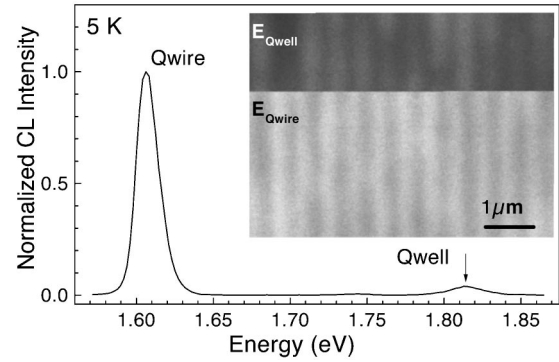


FIG. 1. CL spectrum and CL image of a stacked Qwire array on GaAs(311)A substrate at 5 K. For the upper (lower) part of the CL image, the detection energy was set to the Qwell (Qwire) CL line of the spectrum.

any Qwire related contrast in the CL micrograph. One reason for a reduced exciton transfer efficiency at low temperatures could be the localization of excitons within the Qwell regions due to potential fluctuations. This contribution is less relevant at higher temperatures. Consequently, the CL contrast decreases with increasing temperature.<sup>15</sup>

Figure 2 displays a CL spectrum and a CL micrograph of the Qwire array at room temperature. It contains two important results, which seem to contradict each other. The first one is that we establish a high Qwire luminescence efficiency even at 300 K without notable repopulation of the Qwell regions, which implies a perfect transfer of carriers towards the Qwires. The second one is that a strong wire-related CL contrast clearly re-appears again at room temperature, which implies a nonperfect carrier transfer between Qwell and Qwire regions. This contradiction led us to a more detailed investigation of the loss mechanisms, which can be responsible for a reduced transfer efficiency in these Qwire structures.

In Figs. 1 and 2, the ratio  $R_{PL}$  of the spatially integrated CL intensities of the Qwell and Qwire spectra is 0.05 and smaller than 0.01, respectively. From this point of view, we would conclude that for  $T=5 \text{ K}$  about 95% and for  $T=300 \text{ K}$  almost 100% of the excitons are found within the Qwires before radiative recombination takes place. Since this

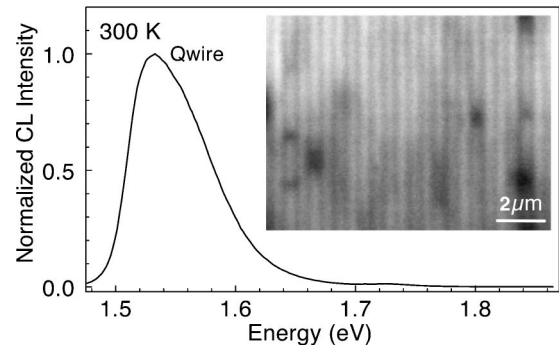


FIG. 2. CL spectrum and CL image of a stacked Qwire array on GaAs(311)A substrate at 300 K. The detection energy is set to the maximum position of the CL spectrum. Note the strong Qwire related CL contrast in the CL micrograph, although the Qwell CL has almost completely disappeared.

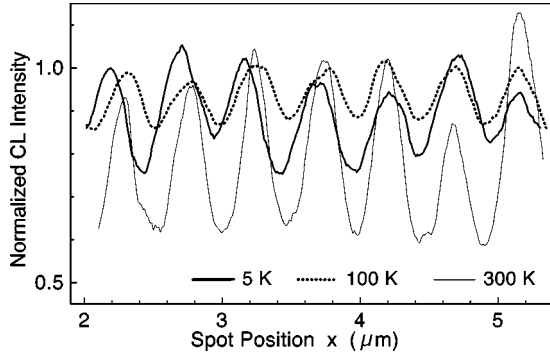


FIG. 3. Normalized CL line profiles perpendicular to the wires of a stacked Qwire array at different temperatures. The respective detection energy is set to the maximum position of the wire line.

estimate neglects nonradiative recombination channels, we will discuss another approach to estimate the transfer rate or efficiency, which is based upon spatially resolved measurements of the Qwire CL intensity. The idea is to generate the excitons within a small limited volume of the Qwell regions and to detect the portion, which recombines radiatively within the Qwires. This approach is realized by recording the Qwire CL intensity, while the electron beam scans along a line perpendicular to the Qwires, i.e., by measuring line profiles of the Qwire CL intensity. Provided that the scattering length of the exciting electrons is smaller than the wire period (for an electron beam position centered between two wires, direct excitation of the wire regions is avoided), the value of the maximum CL contrast  $C = 1 - I_{min}^R / I_{max}^R$ , where  $I_{min}^R$  and  $I_{max}^R$  denote the minimum and maximum intensities of the Qwire CL line profile, is controlled by exciton diffusion. Therefore,  $C$  can be considered as a measure for the transfer efficiency of excitons generated in the Qwell regions. The more efficient the exciton transfer is, the smaller the value of  $C$ . Since the transfer efficiency is a function of the beam position  $x$ , we consider the maximum contrast  $C$  as a measure for the minimum exciton transfer efficiency and  $\bar{C}$  averaged over all the positions along the line ( $\bar{C}$ ) as a measure for the mean transfer efficiency.

Line profiles of the Qwire CL recorded at 5, 100, and 300 K are shown in Fig. 3. The diameter of the electron scattering sphere amounts to about 200 nm for the chosen value of the acceleration voltage of 5 kV. Since the connecting Qwell regions are more than two times wider,  $C$  is controlled by exciton diffusion and thus directly related to the transfer efficiency. For a comparison with the intensity ratio  $R_{PL}$ , we focus first on the line profile obtained at 5 K. The corresponding contrast values are determined to be  $C = 0.2$  and  $\bar{C} \geq 0.15$ , where  $C$  is the average value of all adjacent extrema in the line profile. We conclude that at 5 K less than 85% of the excitons are found within the Qwires before radiative recombination takes place. The difference to the value of 95% obtained by the ratio  $R_{PL}$  can originate from nonradiative recombination within the Qwell regions. The exciton diffusion length  $L$  and thus the transfer efficiency depend on the excitonic diffusivity  $D$  as well as on the nonradiative and radiative lifetimes  $\tau_{nr}$  and  $\tau_r$ , respectively. It can be written as

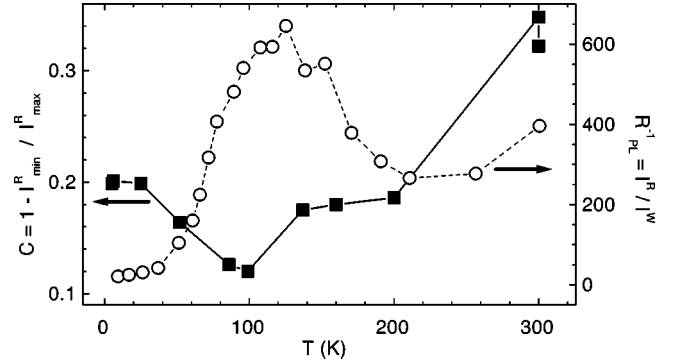


FIG. 4. Temperature dependence of the CL contrast  $C$  (squares) and the ratio  $R_{PL}^{-1}$  (circles) of the spatially integrated intensities of the Qwire and Qwell CL. The contrast was measured by CL line scans.

$$L = \sqrt{D\tau}, \quad \text{where} \quad \frac{1}{\tau} = \frac{1}{\tau_r} + \frac{1}{\tau_{nr}}. \quad (1)$$

Both  $D$  and  $\tau$  vary with  $T$  resulting in a temperature dependent transfer efficiency, which is clearly reflected by the different modulation depths of the line profiles in Fig. 3. Detailed experimental data for  $D(T)$  and  $\tau(T)$  of Qwells with different well widths were reported by Hillmer *et al.*<sup>14</sup> and Gurioli *et al.*<sup>10</sup>, respectively. In order to decide, which of the values  $D$ ,  $\tau_{nr}$ , or  $\tau_r$  actually controls  $L$ , we measured  $C(T)$  over the whole temperature range between 5 and 300 K. In Fig. 4, the corresponding results are indicated as squares. The circles denote the inverse of the ratio  $R_{PL}$  as a function of  $T$ . Starting at 5 K, the value of  $C$  drops with increasing  $T$ , until 100 K is reached. At the same time,  $R_{PL}^{-1}$  increases strongly.  $C$  increases again for  $T > 100$  K showing a drastic enhancement between 200 and 300 K. Taking into account the results of Hillmer *et al.*<sup>14</sup> and Gurioli *et al.*<sup>10</sup> for comparable well widths, the decrease and increase of  $C$  and  $R_{PL}^{-1}$  between 4 and 100 K, respectively, are probably due to an increase of both, the exciton diffusivity and the lifetime. Since for  $T > 100$  K it is not expected that the diffusivity drops to values comparable to those at 5 K, the contribution of  $D$  to the increase of  $C$  is probably small in this temperature range. Therefore, the re-appearance of the CL contrast above 100 K is mainly governed by the  $T$  dependence of the exciton lifetime, which is consistent with the minimum position of  $C$  at 100 K, where Gurioli *et al.* found a maximum of  $\tau$  for 2 nm thick Qwells.<sup>10</sup> Furthermore, since the reduction of the lifetime for  $T > 100$  K can only originate from the nonradiative contribution (the radiative lifetime increases continuously with increasing temperature<sup>10,16</sup>), the observed  $T$  dependence of  $C$  indicates the presence and influence of nonradiative recombination channels within the Qwell regions. Therefore, we assume that besides exciton localization nonradiative recombination can contribute to the reduction of the transfer efficiency even at low temperatures. This nonradiative contribution can vary from sample to sample due to the different growth conditions. Hence, nonradiative recombination of excitons within the connecting Qwell regions is a limiting process for the transfer efficiency at least for temperatures between 5 and 200 K. The behavior of  $R_{PL}^{-1}$  for  $T$

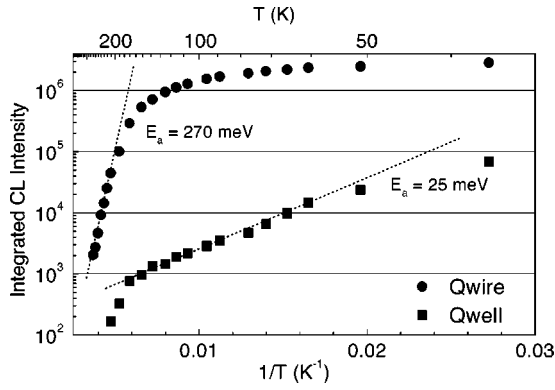


FIG. 5. Temperature dependence of the integrated CL intensities originating from the Qwire (circles) and connecting Qwell (squares) regions. The dashed lines describe an exponential temperature dependence with the respective activation energy ( $E_a$ ).

>150 K and the drastic increase of  $C$  for  $T > 200$  K will be discussed in the following subsection.

### B. Loss mechanisms at elevated temperatures

For values of  $T$  near room temperature, additional mechanisms, which result in a loss of Qwire excitons, have generally to be taken into account. Since at 300 K the thermal energy reaches values comparable with the excitonic binding energy, exciton dissociation should be taken into account. Nevertheless, as has already been shown previously, the majority of the confined excitons is expected to remain in the excitonic state even at 300 K.<sup>17,18</sup>

The comparison of the temperature dependencies of  $C$  and  $R_{PL}^{-1}$  in Fig. 4 as well as of the integrated Qwell and Qwire CL intensities in Fig. 5 gives insight in additional thermally activated loss mechanisms. Figure 5 shows that both, the Qwire and Qwell CL intensity, decrease continuously with increasing  $T$ . Moreover, between 50 and 150 K, the Qwell CL intensity decreases exponentially with a thermal activation energy ( $E_a$ ) of about 25 meV. Since for the chosen growth conditions, the migration length of the Ga adatoms is larger than the period of the Qwire array, the evolution of thinner Qwell regions near the Qwires acting as potential barriers is not expected. Therefore, we conclude that in the sub-micron Qwire array, the thermally activated increase of the transfer efficiency is attributed rather to exciton delocalization than to thermally activated overcoming of a potential barrier between Qwire and Qwell regions as has recently been found for single Qwires fabricated under comparable conditions.<sup>19,20</sup> This conclusion is consistent with the extracted value of  $E_a$ , which is typical for potential fluctuations within the connecting Qwells due to monolayer variations of the well thickness.<sup>18</sup> For temperatures exceeding 150 K,  $R_{PL}^{-1}$  firstly decreases and then increases again for values of  $T$  near 300 K. The increase of  $C$  and  $R_{PL}^{-1}$  between 200 and 300 K coincides with a strong reduction of the Qwire CL intensity within the same temperature range (cf. Fig. 5). These experimental results can be explained, when the escape of excitons out of the Qwire and Qwell regions is taken into account. The potential barrier ( $E_l$ ), which has to be overcome by excitons, in order to be released out of the Qwires into the connecting Qwell regions, corresponds to the

energy separation between the Qwell and Qwire lines, which amounts to about 210 meV. However, the potential barrier  $E_v$  for a vertical escape of an exciton as a whole entity out of the Qwell and Qwire into the (Al,Ga)As matrix is expected to be larger than 300 meV. For this estimate, we neglected the probability that electrons can be scattered into the X band of the (Al,Ga)As matrix, which for the chosen AIAs mole fraction (0.5) is lower in energy than the  $\Gamma$  band. Moreover,  $E_v$  is much smaller for the Qwells than for the Qwires. Therefore, the vertical escape probability is expected to be much higher within the Qwell regions.

Using the information given above, we tentatively discuss the experimental data of Figs. 4 and 5 as follows. Since for  $T > 100$  K the increase of  $C$  is assigned to nonradiative recombination within the Qwells, it cannot be linked to the decrease of  $R_{PL}^{-1}$ . Moreover, the onset of the reduction of  $R_{PL}^{-1}$  is shifted towards higher temperatures compared with the one of the contrast increase. Therefore, the decrease of  $R_{PL}^{-1}$  for  $T > 150$  K indicates most probably a lateral escape of excitons out of the Qwire regions. In consideration of the value of  $E_l$ , the corresponding repopulation of the connecting Qwells is expected to be smaller than 1% under thermal equilibrium conditions, which is consistent with the minimum value of  $R_{PL}^{-1}$  between 200 and 300. The fraction of Qwire excitons, which are thermally emitted into the Qwells, has been found to be remarkably larger for Qwires exhibiting a smaller lateral confinement potential compared with the Qwire system investigated in this work.<sup>8</sup> The fact that  $R_{PL}^{-1}$  increases again for  $T > 200$  K as well as the strongly increased value of  $C$  at 300 K indicate the presence of additional losses, in particular within the Qwell regions for  $T$  near room temperature. These losses are obviously connected with the steep decrease of the integrated Qwire CL intensity within the same temperature range (cf. Fig. 5). From the estimated thermal activation energy of about 270 meV, which is of similar magnitude as  $E_v$  of the Qwells, we conclude that at temperatures near 300 K preferred exciton re-emission out of the connecting Qwell regions into the (Al,Ga)As barriers is mainly responsible for both, an overall carrier loss and an increase of  $C$ . Since the (Al,Ga)As barrier material usually builds a reservoir of several kinds of carrier traps acting as nonradiative recombination centers,<sup>21–24</sup> whose densities are particularly high at the heterointerfaces<sup>25</sup> and which increase with increasing AIAs mole fraction, the vertical escape of carriers into the barrier matrix can be considered as a very effective loss mechanism. The lateral carrier escape solely leads to a thermal equilibrium distribution between Qwire and Qwell regions, whereby the corresponding repopulation of the Qwell regions is limited by the lateral confinement energy.

### C. Time-resolved PL

Figure 6 shows transients of the PL intensity for the Qwire and Qwell PL measured at 5 K in the wire array and unpatterned reference sample. The temporal decay of the Qwell PL follows a single exponential over a wide time range for both, the patterned and unpatterned sample, indicating decay times ( $\tau$ ) of 250 ps and 340 ps, respectively. This difference cannot be attributed to the thinner Qwell layer in the Qwire array compared with the reference

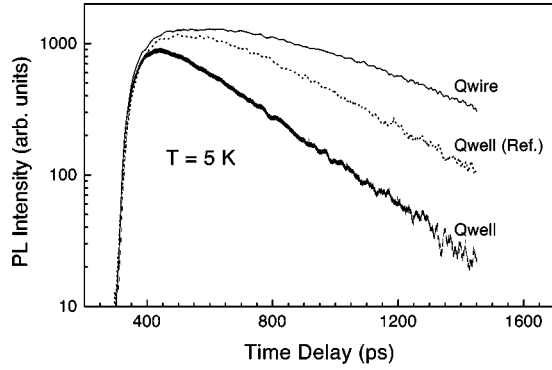


FIG. 6. Time dependence of the PL intensity obtained from the Qwire and Qwell regions of the wire array and from the reference Qwell at 5 K.

Qwell—the decay time is found to be almost independent on the Qwell thickness ( $L_z$ ), when  $L_z$  is smaller than about 15 nm<sup>10,26</sup>—but reflects the influence of the exciton transfer from the Qwell to the Qwire regions resulting in the faster decay compared with the reference sample. Hence, the measured decay time of the Qwell PL provides the total exciton decay rate within the connecting wells, including radiative and nonradiative recombination as well as the exciton transfer. With regard to the Qwire PL, the exciton transfer results in a delayed onset of the decay by about 250 ps. Moreover, an exponential decay can only be observed after about 900 ps resulting in a value of  $\tau \approx 450$  ps. This part of the Qwire transient is a result of the radiative and nonradiative recombination rates within the wires. The delayed onset of the PL decay in the unpatterned reference Qwell is attributed to the high energy level of the used laser mode resulting in a very small excitation depth. The subsequent carrier motion from the excited surface layer down to the Qwells causes a delay (in particular, at low  $T$ ), which in the patterned sample increased for the Qwires and decreased for the Qwells. The statements about the exciton decay rates are in principal valid only at low temperatures.

In the following, a model is proposed, which enables us to estimate the exciton transfer time as well as the ratio of the radiative lifetimes in the Qwell and Qwire regions by combining the results of spatially and time-resolved experiments.

#### D. Model

The exciton rates  $\Gamma$ , which are important for the recombination behavior of a Qwire/Qwell array, are illustrated in Fig. 7.  $\Gamma_r^W$ ,  $\Gamma_{nr}^W$ ,  $\Gamma_r^R$ , and  $\Gamma_{nr}^R$  denote the radiative and nonradiative recombination rates within the Qwell and Qwire regions, respectively.  $\Gamma_t(x)$ ,  $\Gamma_l$ , and  $\Gamma_v$  are the transfer rate of the excitons from the connecting Qwell towards the Qwire regions and the lateral as well as vertical escape rates of excitons out of the Qwires into the Qwell regions and out of the Qwells into the (Al,Ga)As barrier material, respectively. The total rate in the Qwell regions  $\Gamma^W$  consists of the following components:

$$\Gamma^W = \Gamma_r^W + \Gamma_{nr}^W + \overline{\Gamma}_t + \Gamma_v - \frac{1}{f} \Gamma_l, \quad (2)$$

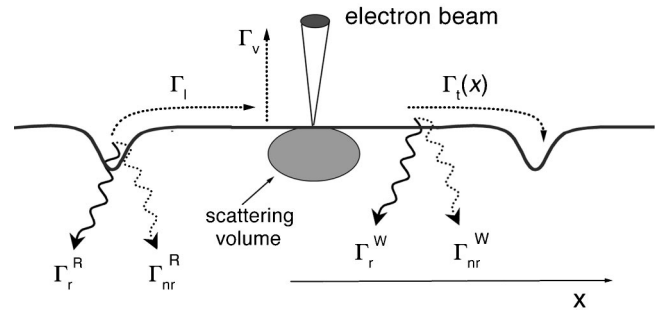


FIG. 7. Sketch of the CL line profile measurement.  $\Gamma_r^R$ ,  $\Gamma_{nr}^R$ ,  $\Gamma_r^W$ , and  $\Gamma_{nr}^W$  denote the radiative and nonradiative recombination rates within the Qwire and Qwell regions, respectively.  $\Gamma_l$ ,  $\Gamma_v$ , and  $\Gamma_t(x)$  are the lateral escape rate out of the Qwire into the Qwell regions, the vertical escape rate out of the Qwell regions into the (Al,Ga)As barriers, and the exciton transfer rate, respectively.

where  $\overline{\Gamma}_t$  is the averaged transfer rate and  $f = w/r$  the ratio of the lateral Qwell and Qwire widths. The factor  $1/f$  in Eq. (2) accounts for the smaller width of the Qwire regions. In the investigated Qwire array,  $\Gamma_l$  and  $\Gamma_v$  become important only at elevated temperatures (near 300 K). Since the experimentally obtained decay rates can only be easily described for low  $T$ , the following consideration refers to low temperatures, and  $\Gamma_l$  as well as  $\Gamma_v$  are negligible.

With regard to the line profiles of the Qwire CL,  $I_R^R$  and  $\overline{I_W^R}$  denote the Qwire CL intensity for excitation within the Qwire and Qwell regions, respectively, where  $\overline{I_W^R}$  is averaged over the lateral width of the Qwell regions. Although the scattering radius of the electron beam is larger than the width of the Qwires, we assume for  $I_R^R$  that most of the carriers excited within the surrounding Qwell regions are able to move to the Qwires before recombination takes place. With this assumption, the averaged CL intensity ratio is

$$R_{CL} \equiv \frac{\overline{I_W^R}}{I_R^R} = \frac{\overline{\Gamma}_t}{\Gamma^W} \quad \text{or} \quad \overline{\Gamma}_t = R_{CL} \times \Gamma^W. \quad (3)$$

$R_{CL}$  is related to the averaged CL contrast by  $\overline{C} = 1 - R_{CL}$ . Note that the Qwire related CL contrast depends only on the rates within the Qwell regions, because the factor  $\Gamma_r^R / (\Gamma_r^R + \Gamma_{nr}^R)$  contained in both, the numerator and denominator of Eq. (3), cancels.

The inverse of  $\overline{\Gamma}_t$  can be considered as an effective transfer time  $\tau_t^{eff} = \tau^W / R_{CL}$ , where  $\tau^W = 1/\Gamma^W$  denotes the total decay time in the connecting wells. Consequently, the exciton transfer rate can be determined by measuring the Qwire related CL contrast and the decay rate of the Qwell luminescence intensity. The experimental data obtained at 5 K ( $R_{CL} = 0.85$ ,  $\tau^W = 250$  ps) result in a transfer time of  $\tau_t^{eff} \approx 300$  ps, which is much larger than previously estimated.<sup>2</sup> However, since for thin Qwells and at low temperatures the diffusion length within the excitonic lifetime is expected to be on the order of a few 100 nm, which is of similar magnitude as the wire period, it is not surprising that  $\tau_t^{eff}$  is very similar to the lifetime in unstructured Qwells. Exciton localization due to potential fluctuations is the most effective mechanism, which contributes to a reduced transfer rate in particular for thinner Qwells and at lower temperatures. Nev-

ertheless, the Qwire luminescence intensity dominates remarkably over the Qwell intensity even at 5 K, where  $R_{PL} = 0.05$ . Since the luminescence efficiency of the wire array is not only controlled by the transfer rate, but also by the ratio of the radiative and non-radiative recombination rates within the Qwire and Qwell, we will now discuss the ratio  $R_{PL}$  in terms of the recombination and transfer rates.

The spatially integrated luminescence intensity of the Qwires can be written as a sum of the radiatively recombining fraction of the excitons, which are excited within the Qwire regions and those, which are excited within the Qwell regions and subsequently transferred to the Qwires

$$\begin{aligned} I_{PL}^R &= I_0 \frac{\Gamma_r^R}{\Gamma_r^R + \Gamma_{nr}^R} \left( r + \frac{\bar{\Gamma}_t}{\bar{\Gamma}^W w} \right) \\ &= I_0 \frac{\Gamma_r^R}{\Gamma_r^R + \Gamma_{nr}^R} (r + w R_{CL}). \end{aligned} \quad (4)$$

The spatially integrated luminescence intensity of the Qwells consists (at least for low  $T$ ) solely of the radiatively recombining fraction of the excitons, which are excited in the Qwell regions

$$\begin{aligned} I_{PL}^W &= I_0 \frac{\Gamma_r^W}{\Gamma_r^W + \Gamma_{nr}^W} w \left( 1 - \frac{\bar{\Gamma}_t}{\bar{\Gamma}^W} \right) \\ &= I_0 \frac{\Gamma_r^W}{\Gamma_r^W + \Gamma_{nr}^W} w (1 - R_{CL}). \end{aligned} \quad (5)$$

Using the inverse of  $R_{PL}$ , namely  $R_{PL}^{-1} = I_{PL}^R / I_{PL}^W$ , we obtain the following relation between the radiative and non-radiative recombination rates within the Qwells and Qwires

$$\frac{R_{PL}^{-1}}{F_{CL}} \times \frac{\Gamma_r^W}{\Gamma_r^W + \Gamma_{nr}^W} = \frac{\Gamma_r^R}{\Gamma_r^R + \Gamma_{nr}^R}, \quad (6)$$

where

$$F_{CL} = \frac{1/f + R_{CL}}{\bar{C}}. \quad (7)$$

Equation (6) contains data from laterally integrated ( $R_{PL}^{-1}$ ) as well as from spatially resolved ( $F_{CL}$ ) experiments. In order to estimate the relation between the radiative rates of the Qwell and Qwire regions, we need to add the information provided by the time-resolved experiments.

The temporal variation of the exciton concentration ( $N_R$ ) within the Qwires after excitation by an ultrashort pulse is determined by the decay rate  $\Gamma^R = \Gamma_r^R + \Gamma_{nr}^R$  within the Qwires as well as by the exciton transfer from the Qwells, which again depends on the transfer rate  $\Gamma_t$  and on the decay rate  $\Gamma^W$  within the Qwell regions. Hence,  $\dot{N}_R = dN_R/dt$  can be written as

$$\dot{N}_R = -\Gamma^R N_R + f \bar{\Gamma}_t N_0 e^{-\Gamma^W t}, \quad (8)$$

where  $N_0$  denotes the exciton concentration immediately after excitation. Its solution is

$$\frac{N_R(t)}{N_0} = \frac{\Gamma^W R_{CL} f}{\Gamma^R - \Gamma^W} \times e^{-\Gamma^W t} + \left( 1 - \frac{\Gamma^W R_{CL} f}{\Gamma^R - \Gamma^W} \right) \times e^{-\Gamma^R t}, \quad (9)$$

where  $\bar{\Gamma}_t$  was replaced by  $R_{CL} \times \Gamma^W$  [cf. Eq. (3)]. Since high transfer rates are desirable,  $\Gamma^W$  should be much larger than  $\Gamma^R$ . Hence, the contribution of the first part of Eq. (9) disappears faster than the second one. Consequently, for large values of  $t$ , the transient slope of the Qwire PL is mainly determined by  $\Gamma^R$ , and the experimentally obtained decay rate  $\Gamma_{exp}^R(t \rightarrow \infty) = \Gamma_{\infty}^R$  can be assigned to  $\Gamma_r^R + \Gamma_{nr}^R$ . Together with Eqs. (2) and (3), Eq. (6) can be written as

$$\frac{\tau_r^W}{\tau_r^R} = \frac{\tau^W}{\tau_{\infty}^R R_{PL} (f^{-1} + R_{CL})}. \quad (10)$$

This equation implies that a combination of time- and spatially resolved luminescence experiments enables us to determine the ratio of the radiative recombination times of the Qwires and Qwells in coupled Qwire/Qwell structures. With our experimentally obtained data at 5 K,  $R_{PL}^{-1} = 20$ ,  $F_{CL} \approx 6$ ,  $\bar{C} = 0.15$ ,  $\tau_{\infty}^R = 450$  ps, and  $\tau^W = 250$  ps, we obtain  $\tau_r^W / \tau_r^R = 12$ , which is very surprising, since for the respective lifetime ratio of independent Qwells and Qwires the inverse ( $\tau_r^R / \tau_r^W \approx 10$ ) is expected.<sup>16</sup> Further effort is necessary to clarify the reason for the experimentally found small contribution of the radiative recombination within the connecting Qwells compared with the one in the Qwires. Hence, future work will focus on the combination of spatially and time-resolved experiments in such systems, in particular, with different lateral and vertical Qwell widths. However, the discussion of our experimental results reflects a very interesting fact: namely that a small ratio of the PL intensities from the Qwell and Qwire regions does not necessarily imply a high transfer rate, but can also be due to remarkably different recombination rates.

#### IV. SUMMARY

The high growth selectivity on GaAs(311)A substrates patterned by a sub- $\mu\text{m}$ -pitch grating results in geometrically flat quantum wire arrays with lateral confinement potentials, which are as high as 210 meV. Consequently, the exciton capture within the wire regions is very efficient, and high wire luminescence intensities are obtained up to room temperature. The combined measurement of the wire related CL contrast  $C$  and the ratio of the laterally integrated intensities of the quantum well and wire luminescence as a function of temperature yields important information about the exciton transfer between the connecting Qwell regions and the Qwires, about the influence of nonradiative recombination channels, and about the thermally activated carrier escape. At low temperatures (5–20 K) both, exciton localization and nonradiative recombination, contribute to a reduced exciton transfer efficiency. While the exciton transfer is nearly complete at about 100 K, which is linked to the maximum of the exciton lifetime in this temperature range, it is reduced again for  $T > 100$  K due to an increase of the nonradiative recom-

bination rate in the well regions. The decrease of the Qwire luminescence intensity as well as the remarkable increase of  $C$  near room temperature is attributed to a vertical carrier escape, in particular out of the quantum well regions into the (Al,Ga)As barriers. The exciton transfer time and the ratio of the radiative recombination rates in the well and wire regions can be obtained, when the spatially resolved are combined with time-resolved measurements.

## ACKNOWLEDGMENTS

The authors would like to thank Th. Kurth and D. Heitmann, University Hamburg, for performing the holographic lithography and P. Santos for valuable discussions and a critical reading of the manuscript. This work was supported in part by the Bundesministerium für Bildung, Wissenschaft, Forschung und Technologie.

- 
- <sup>1</sup>M. Walther, E. Kapon, J. Christen, D. M. Hwang, and R. Bhat, *Appl. Phys. Lett.* **60**, 521 (1992).
- <sup>2</sup>J. Christen, M. Grundmann, E. Kapon, E. Colas, D. M. Hwang, and D. Bimberg, *Appl. Phys. Lett.* **61**, 67 (1992).
- <sup>3</sup>M. Walther, E. Kapon, C. Caneau, D. M. Hwang, and L. M. Schiavone, *Appl. Phys. Lett.* **62**, 2170 (1993).
- <sup>4</sup>M. Grundmann, J. Christen, M. Joschko, O. Stier, D. Bimberg, and E. Kapon, *Semicond. Sci. Technol.* **9**, 1939 (1994).
- <sup>5</sup>A. Gustafsson, F. Reinhardt, G. Biasiol, and E. Kapon, *Appl. Phys. Lett.* **67**, 3673 (1995).
- <sup>6</sup>R. Nötzel, M. Ramsteiner, J. Menniger, A. Trampert, H.-P. Schönherr, L. Däweritz, and K. H. Ploog, *J. Appl. Phys.* **80**, 4108 (1996).
- <sup>7</sup>J. F. Ryan, A. C. Maciel, C. Kiener, L. Rota, K. Turner, J. M. Freyland, U. Marti, D. Martin, F. Morier-Gemoud, and F. K. Reinhart, *Phys. Rev. B* **53**, R4225 (1996).
- <sup>8</sup>A. Richter, G. Behme, M. Süptitz, Ch. Lienau, T. Elsaesser, M. Ramsteiner, R. Nötzel, and K. H. Ploog, *Phys. Rev. Lett.* **79**, 2145 (1997).
- <sup>9</sup>W. Pan, H. Yaguchi, Y. Hanamaki, M. Ishikawa, Y. Kaneko, K. Onabe, R. Ito, and Y. Shiraki, *J. Cryst. Growth* **170**, 585 (1997).
- <sup>10</sup>M. Gurioli, A. Vinattieri, M. Colocci, C. Deparis, J. Massies, G. Neu, A. Bosacchi, and S. Franchi, *Phys. Rev. B* **44**, 3115 (1991).
- <sup>11</sup>Y. J. Ding, C. L. Guo, S. Li, B. Khurgin, K.-K. Law, and J. Merz, *Appl. Phys. Lett.* **60**, 154 (1992).
- <sup>12</sup>A. Fujiwara, K. Muraki, S. Fukatsu, Y. Shiraki, and R. Ito, *Phys. Rev. B* **51**, 14 324 (1995).
- <sup>13</sup>S. T. Pérez-Merchancano, M. de Dios-Leyva, and L. E. Oliveira, *J. Appl. Phys.* **81**, 7945 (1997).
- <sup>14</sup>H. Hillmer, A. Forchel, C. W. Tu, and R. Sauer, *Semicond. Sci. Technol.* **7**, B235 (1992).
- <sup>15</sup>R. Nötzel, U. Jahn, Z. Niu, A. Trampert, J. Fricke, H.-P. Schönherr, T. Kurth, D. Heitmann, L. Däweritz, and K. H. Ploog, *Appl. Phys. Lett.* **72**, 2002 (1998).
- <sup>16</sup>D. S. Citrin, *Phys. Rev. Lett.* **69**, 3393 (1992).
- <sup>17</sup>M. Colocci, M. Gurioli, and A. Vinattieri, *J. Appl. Phys.* **68**, 2809 (1990).
- <sup>18</sup>M. A. Herman, D. Bimberg, and J. Christen, *J. Appl. Phys.* **70**, R1 (1991).
- <sup>19</sup>Ch. Lienau, A. Richter, G. Behme, M. Süptitz, D. Heinrich, T. Elsaesser, M. Ramsteiner, R. Nötzel, and K. H. Ploog, *Phys. Rev. B* **58**, 2045 (1998).
- <sup>20</sup>A. Richter, M. Süptitz, D. Heinrich, Ch. Lienau, T. Elsaesser, M. Ramsteiner, R. Nötzel, and K. H. Ploog, *Appl. Phys. Lett.* **73**, 2176 (1998).
- <sup>21</sup>K. Yamanaka, S. Naritsuka, M. Mannoh, T. Yuasa, Y. Nomura, M. Mihara, and M. Ishii, *J. Vac. Sci. Technol. B* **2**, 229 (1984).
- <sup>22</sup>K. Akimoto, M. Kamada, K. Taira, M. Arai, and N. Watanabe, *J. Appl. Phys.* **59**, 2833 (1986).
- <sup>23</sup>K. Yamanaka, S. Naritsuka, K. Kanamoto, M. Mihara, and M. Ishii, *J. Appl. Phys.* **61**, 5062 (1987).
- <sup>24</sup>K. Hoshino, T. Uchida, N. Kamata, K. Yamada, M. Nishioka, and Y. Arakawa, *Jpn. J. Appl. Phys.* **37**, 3210 (1998).
- <sup>25</sup>P. Krispin, R. Hey, and H. Kostial, *J. Appl. Phys.* **77**, 5773 (1995).
- <sup>26</sup>J. Martinez-Pastor, A. Vinattieri, L. Carraresi, M. Colocci, Ph. Roussignol, and G. Weimann, *Phys. Rev. B* **47**, 10 456 (1993).